Characteristics of Nickel(0), Nickel(I), and Nickel(II) in Phosphino Thioether Complexes: Molecular Structure and *S*-Dealkylation of $(Ph_2P(o\text{-}C_6H_4)SCH_3)_2Ni^0$

Jang Sub Kim, Joseph H. Reibenspies, and Marcetta Y. Darensbourg*

Contribution from the Department of Chemistry, Texas A&M University, College Station, Texas 77843

Received November 1, 1995[⊗]

Abstract: The molecular structure of a nickel(0) complex with P,S-donor atom ligands has been characterized by X-ray crystallography. Complex **1**, $(Ph_2P(o\text{-}C_6H_4)SCH_3)_2Ni^0$, prepared by Na/Hg amalgam reduction of the Ni^{II} complex $[(Ph_2P(o\text{-}C_6H_4)SCH_3)_2Ni](BF_4)_2$ ($[2](BF_4)_2$), degrades photochemically with loss of CH_3 radicals to yield complex **3**, $(Ph_2P(o\text{-}C_6H_4)S)_2Ni^{II}$. Crystallographic parameters for the three compounds are as follows: **1**, monoclinic space group $C2/c$ with $a = 11.467(2)$ Å, $b = 17.613(3)$ Å, $c = 15.733(2)$ Å, $\beta = 96.450(10)°$, $V = 3157.5(9)$ Å^3, and $Z = 4$; $[2](BF_4)_2$, monoclinic space group $P2_1/c$ with $a = 9.417(4)$ Å, $b = 14.822(9)$ Å, $c = 13.773(2)$ Å, $\beta = 98.55(3)°$, $V = 9101(14)$ Å^3, and $Z = 2$; and **3**, monoclinic space group $P2_1/c$ with $a = 9.651(2)$ Å, $b = 12.971(8)$ Å, $c = 12.540(2)$ Å, $\beta = 110.46(2)°$, $V = 1470.7(11)$ Å^3, and $Z = 2$. While complex **1** has a distorted tetrahedral geometry, complexes $[2](BF_4)_2$ and **3** are square planar with *trans* stereochemistry. The cyclic voltammogram of $[2](BF_4)_2$ in CH_3CN shows two redox events assigned to $Ni^{II/I}$ and $Ni^{I/0}$, whereas the thiolate **3** reveals only one reversible wave assigned to $Ni^{II/III}$. The chemical reduction of $[2](BF_4)_2$ with Cp_2Co provided a Ni^I species, $[(Ph_2P(o\text{-}C_6H_4)SCH_3)_2Ni^I]^+$, characterized at 100 K by an axial EPR signal with $g_x = g_y = 2.10$ and $g_z = 1.96$. Hyperfine spectral features resulting from coupling to two ^{31}P nuclei suggests a retention of substantially square planar geometry. In contrast the isotropic character of the EPR signal of $[(Ph_2P(o\text{-}C_6H_4)SCH_3)(Ph_2P(o\text{-}C_6H_4)S)Ni^I]$, presumed to be the first product of the photochemical demethylation of **1** ultimately yielding the doubly demethylated complex **3**, suggested the intervening thioether/thiolate Ni^I species to be pseudotetrahedral. Protonation of the nickel(0) species **1** produced a five-coordinate nickel hydride complex, $[(H)(arom\text{-}PSMe)_2Ni]BF_4$, **4**.

Introduction

Group VIII metal complexes of N,S, P,S, and As,S donor chelates have been extensively studied for their ability to transfer alkyl groups from sulfur to suitable nucleophiles.[1−3] Such alkyl transfers from nickel(II) and palladium(II) complexes of the *o*-(diphenylphosphino)thioanisole ligand ($Ph_2P\text{-}o\text{-}C_6H_4SMe$, designated hereafter as arom-PSMe) to amines have been characterized as Menschutkin type S_N2 reactions.[3b,4] Roundhill and Benefiel have provided kinetic monitors of reaction (eq 1), demonstrating bimolecular kinetic behavior with $\Delta H^{\ddagger}$ in the range of $+13$ to $+19$ kcal mol^{-1} and $\Delta S^{\ddagger}$ in the range of -14 to -30 cal K^{-1} mol^{-1}.[5] (Note: The representation of *cis* stereochemistry for $(Ph_2P\text{-}o\text{-}C_6H_4SEt)_2Pt^{II}$ is as suggested by

(1)
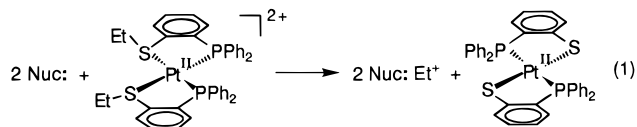
Roundhill and Benefiel.[5] In contrast the two known structures of bidentate phosphino thioether derivatives of Ni^{II} are *trans*.).[6]

With this history of nucleophilic displacement of *S*-alkyls, the instability of the iodide salt of $[(arom\text{-}PSMe)_2Ni](I)_2$, $[2](I)_2$, was readily rationalized according to eq 2, and our goal of isolating and chemically characterizing a nickel(0) complex, **1**, $[(arom\text{-}PSMe)_2Ni^0]$, necessitated the synthesis of the BF_4^- salt, described by eq 3. This salt was successfully used in the

(2)

$$2\ arom\text{-}PSMe + Ni(BF_4)_2 \cdot 6\ H_2O \xrightarrow{i\text{-}PrOH} [(arom\text{-}PSMe)_2Ni](BF_4)_2 \quad (3)$$
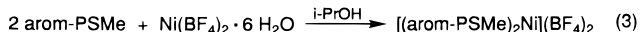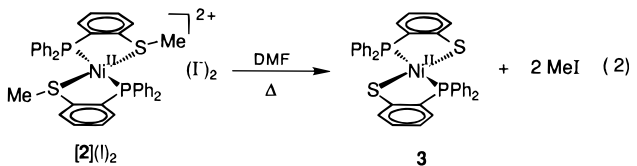
preparation and isolation of **1**. Its molecular structure, presented below, is the first nickel(0) complex ligated by phosphorus and sulfur donor atoms whose structure has been determined by X-ray crystallography. (The assumption of tetrahedral geometry for a similar P_2S_2Ni complex was recently expressed in work which similarly detailed nickel redox properties with complex

[⊗] Abstract published in *Advance ACS Abstracts,* April 15, 1996.

(1) (a) Hay, R. W.; Galyer, A. L.; Lawrance, G. A. *J. Chem. Soc., Dalton Trans.* **1976**, 939. (b) Sacconi, L.; Speroni, G. P. *Inorg. Chem.* **1968**, *7*, 295. (c) Lindoy, L. F.; Livingstone, S. E.; Locker, T. N. *Aust. J. Chem.* **1967**, *20*, 471.

(2) (a) Lindoy, L. F.; Livingstone, S. E.; Locker, T. N. *Inorg. Nucl. Chem. Lett.* **1967**, *3*, 35. (b) Eller, P. G.; Riker, J. M.; Meek, D. W. *J. Am. Chem. Soc.* **1973**, *95*, 3540. (c) Roundhill, D. M.; Beaulieu, W. B.; Bagchi, U. *J. Am. Chem. Soc.* **1979**, *101*, 5428. (d) Roundhill, D. M.; Roundhill, S. G. N.; Beaulieu, W. B.; Bagchi, U. *Inorg. Chem.* **1980**, *19*, 3365. (e) Benefiel, A.; Roundhill, D. M.; Fultz, W. C.; Rheingold, A. L. *Inorg. Chem.* **1984**, *23*, 3316.

(3) (a) McAuliffe, C. A. *Inorg. Chem.* **1973**, *12*, 2477. (b) Dutta, R. L.; Meek, D. W.; Busch, D. H. *Inorg. Chem.* **1970**, *9*, 1215. (c) Dutta, R. L.; Meek, D. W.; Busch, D. H. *Inorg. Chem.* **1970**, *9*, 2098. (d) Lindoy, L. F.; Livingstone, S. E.; Locker, T. N. *Inorg. Chem.* **1967**, *6*, 652. (e) Dutta, R. L.; Meek, D. W.; Busch, D. H. *Inorg. Chem.* **1971**, *10*, 1820.

(4) (a) Menschutkin, N. *Z. Phys. Chem., Stoechim. verwandtschaftsl.* **1890**, *5*, 589. (b) Ingold, C. K. *Structure and Mechanism in Organic Chemistry*; Cornell University Press: Ithaca, NY, 1953; pp 349, 412. (c) Abraham, M. H.; Nasehzadeh, A. *J. Chem. Soc., Chem. Commun.* **1981**, 905. (d) Kevill, D. N. *J. Chem. Soc., Chem. Commun.* **1981**, 421.

(5) Benefiel, A.; Roundhill, D. M. *Inorg. Chem.* **1986**, *25*, 4027.

(6) Hsiao, Y. M.; Chojnacki, S. S.; Hinton, P.; Reibenspies, J. H.; Darensbourg, M. Y. *Organometallics* **1993**, *12*, 870.

geometry.)[7] Interestingly, in the presence of light, the Ni[0] complex **1** also demonstrates instability with respect to methyl group loss, generating the dithiolate complex **3**.

Interest in *S*-alkylation/*S*-dealkylation is currently high as mechanistic knowledge is appropriate both to desulfurization technology[8] and to biological pathways such as methyl transfers from *S*-adenosylmethionine, a natural carbonium ion source, or the methylation dependent functional switch mechanism in the *Escherichia coli* Ada protein.[9,10] That metals might serve to promote bond making as well as bond breaking S–C reactivity is mechanistically challenging, and explorations of first-row metals as candidates for this process provide the impetus for our work. Homolytic S–C bond cleavage reactions are intimately associated with accessibility of low oxidation states,[11,12] and the subsequent partial back-donation of metal electrons into an S–C π* orbital. The work described below combines studies of redox properties, geometry changes, and homolytic S–C activation.

Experimental Section

A. Methods and Materials. All reactions, sample transfers, and sample manipulations were carried out using standard Schlenk techniques (Ar atmosphere) and/or in an argon atmosphere glovebox. [13]CO (99% enriched) was purchased from Cambridge Isotope Laboratory, Inc. Nickel precursors $Ni(BF_4)_2 \cdot 6H_2O$ and $Ni(COD)_2$ (COD = 1,5-cyclooctadiene) were obtained from Strem Chemicals, Inc. All other reagents were commercial products and used as received without further purification. Dichloromethane was distilled over phosphorus pentoxide under nitrogen. Acetone was dried using NaI or dried over molecular sieves (4 Å). Acetonitrile was distilled once from CaH_2, once from P_2O_5, and freshly distilled from CaH_2 and immediately before use. Toluene, benzene, tetrahydrofuran, diethyl ether, and hexane were distilled from sodium/benzophenone ketyl under nitrogen.

B. Instrumentation. Infrared spectra were recorded on a Mattson Galaxy 6021 or an IBM IR/32 using 0.1 mm NaCl sealed cells or KBr pellets. ^{1}H, ^{2}H, ^{13}C, and ^{31}P NMR spectra were obtained on a Varian XL200 spectrometer; all ^{31}P NMR spectra were referenced to PPh3 dissolved in THF and in a sealed capillary tube, which shows a singlet resonance peak at −5.0 ppm referenced to external H_3PO_4. UV–vis spectra were recorded on a Hewlett-Packard 8452A diode array spectrometer. Solution spectra were obtained using 10 mm path length quartz cells.

Cyclic voltammograms were recorded on a BAS-100A electrochemical analyzer using a $Ag/AgNO_3$ reference and glassy carbon working electrodes with 0.1 M [*n*-Bu4N]PF6 electrolyte. All redox potentials were calibrated against ferrocenium $[Cp_2Fe]PF_6$ ($E_{1/2}$ = 400 mV)[13] and referenced to NHE. EPR spectra were recorded on a Bruker ESP 300 equipped with an Oxford ER910A cryostat operating at 10 or 100 K. An NMR gaussmeter (Bruker ERO35M) and Hewlett-Packard frequency counter (HP5352B) were used to calibrate the field and microwave frequency. Samples were first frozen in liquid N_2, and then cooled to a low temperature for analyses. The concentration of paramagnetic nickel(I) species was calculated and compared to the double integral of the EPR spectrum of 1.0 mM Cu(II) in 10.0 mM

EDTA. Photochemical reactions were conducted with a Conrad-Hanovia 450 W Hg vapor lamp with Pyrex sleeves (>360 nm) in a reaction vessel designed for photochemical reaction, all purchased from the Ace Glass Co.

Mass spectra of gas samples generated during the photolysis of **1** were recorded using a VG Analytical 70S high-resolution, double focusing, and sectored mass spectrometer at ionizing energies of 70 eV at the TAMU Center for Chemical Characterization and Analysis. Data were collected by a VG Analytical 11/250J data system. GC/MS of organic samples with high molecular weight were obtained on a Hewlett-Packard, HP, 5890 gas chromatograph with a HP 5971 mass selective detector, and a HP cross-linked methyl silicone capillary column (20 m; 0.20 mm, film thickness 0.33 mm). Elemental analyses were performed by Galbraith Laboratories, Inc., Knoxville, TN.

C. Preparation of Compounds. *o*-**(Diphenylphosphino)thioanisole, ($Ph_2P(o-C_6H_4)SCH_3$, arom-PSMe).** *o*-Aminothioanisole was prepared from the reaction of *o*-mercaptoaniline with sodium followed by iodomethane in methanol.[5] *o*-Iodothioanisole, $I(o-C_6H_4)SCH_3$, and *o*-(diphenylphosphino)thioanisole were prepared by slightly modified literature procedures, and details are given as supporting information.[14–16] Likewise procedures for the preparation of *o*-iodothioanisole-*methyl-d3* ($I(o-C_6H_4)SCD_3$) and *o*-(diphenylphosphino)thioanisole-*methyl-d3* ($Ph_2P(o-C_6H_4)SCD_3$, arom-PSCD3) are deposited as supporting information.

Bis[*o*-(diphenylphosphino)thioanisole]nickel(0) (($(arom-PSMe)_2Ni^0$, 1). Method a. Under an Ar atmosphere, 0.30 g (0.354 mmol) of **2**(BF4)2 in 30 mL of CH_3CN was added to a Na/Hg amalgam (24.0 mg of Na in 1 mL of Hg) in a Schlenk flask and the mixture vigorously stirred for 7 min. The resulting deep red solution was filtered through degassed Celite to remove a precipitated green solid, the amalgam, and NaBF4. Since the solubility of the $(arom-PSMe)_2Ni^0$ product is low in CH_3CN, the Celite was washed with 4 mL of benzene which was also filtered and combined with the CH_3CN filtrate. Methanol (15 mL) was layered on top of the red solution, and the flask was placed in a −5 °C freezer, resulting in the formation of red crystals over the course of 2 days. The red crystals were washed twice with 5 mL of anhydrous diethyl ether and dried under vacuum for 8 h to yield 0.15 g (62%) of **1**. ^{1}H NMR (C_6H_6): δ 7.80–6.80 (m, phenyl, 20 H), 2.18 (s, CH_3, 6H). ^{31}P{^{1}H} NMR (C_6H_6): δ 43.8. Elemental analyses were unreliable presumably due to demethylation, *vide infra*.

Method b. A 50 mL Schlenk flask was charged with 0.10 g (0.364 mmol) of $Ni(COD)_2$ and 0.224 g (0.720 mmol) of arom-PSMe ligand in the Ar-filled glove box. Addition of 15 mL of CH_3CN with vigorous stirring (10 min) gave a red solid which was filtered, washed twice with 15 mL of anhydrous diethyl ether, and dried under vacuum to yield 0.160 g (65%) of **1**. This procedure was also used to produce bis[*o*-(diphenylphosphino)thioanisole-*methyl-d3*]nickel(0) (($(arom-PSCD_3)_2$-Ni^0, **1-d6**), using 0.10 g (36.4 mmol) of $Ni(COD)_2$ and 0.224 g (72.0 mmol) of arom-PSCD3 ligand, yielding 0.20 g (80.7%) of (arom-$PSCD_3)_2Ni^0$. ^{1}H NMR (C_6H_6): δ 7.80–6.80 (m, phenyl, 20 H). ^{31}P{^{1}H} NMR (C_6H_6): δ 43.8.

Bis[*o*-(diphenylphosphino)thioanisole]nickel(II) Bistetrafluoroborate ([($(arom-PSMe)_2Ni$](BF4)2, [2](BF4)2). To a solution of 0.39 g (1.14 mmol) of $Ni(BF_4)_2 \cdot 6H_2O$ in 20.0 mL of 2-propanol was added 0.70 g (2.27 mmol) of the arom-PSMe ligand dissolved in 4.0 mL of THF. The yellow precipitate which formed immediatly was filtered, washed with 10.0 mL of 2-propanol followed by 10.0 mL of THF, and dried under vacuum to yield 0.92 g (95%) of [**2**](BF4)2. ^{1}H NMR (CD_3COCD_3): δ 8.15–7.10 (m, phenyl, 28H), 2.5 (s, CH_3, 6H). ^{31}P{^{1}H} NMR ($CDCl_3$): δ −13.8.

Bis[*o*-(diphenylphosphino)benzenethiolato]nickel(II) (($(arom-PS)_2Ni^{II}$, 3). A mixture of 0.590 g (1.89 mmol) of $Ni(I)_2$ and 1.16 g (3.78 mmol) of arom-PSMe in 30 mL of ethanol (90%) was refluxed for 2 h, resulting in a color change from red-brown to green. The green precipitate which settled out was filtered, washed with 20 mL of CH_3CN followed by 20 mL of diethyl ether, and dried under vacuum to yield 0.70 g (57%) of **3**. ^{1}H NMR ($CDCl_3$): δ 6.85–7.70 (m, C_6H_4,

(7) James, T. L.; Smith, D. M.; Holm, R. H. *Inorg. Chem.* **1994**, *33*, 4869.

(8) (a) Riaz, U.; Curnow, O. J.; Curtis, D. *J. Am. Chem. Soc.* **1994**, *116*, 4357. (b) Robertson, M. J.; Day, C. L.; Jacobson, R. A.; Angelici. R. J. *Organometallics* **1994**, *13*, 179. (c) Benson, J. W.; Angelici, R. J. *Inorg. Chem.* **1993**, *32*, 1871. (d) Benson, J. W.; Angelici, R. J. *Organometallics* **1993**, *12*, 680. (e) Birnbaum, J.; Dubois, M. R. *Organometallics* **1994**, *13*, 1014. (f) Dietz, J. G; Bernatis, P.; Dubois, M. R. *Organometallics* **1993**, *12*, 3630.

(9) Myers, L. C.; Terranova, M. P.; Ferentz, A. E.; Wagner, G.; Verdine, G. L. *Science* **1993**, *261*, 1164.

(10) Ohkubo, T.; Sakashita, H.; Sakuma, T.; Kainosho, M.; Sekiguchi, M.; Morikawa, K. *J. Am. Chem. Soc.* **1994**, *116*, 6035.

(11) Cha, M.; Shoner, S. C.; Kovacs, J. A. *Inorg. Chem.* **1993**, *32*, 1860.

(12) Sellmann, D.; Reisser, W. *J. Organomet. Chem.* **1985**, *297*, 319.

(13) Gagne, R. R.; Koval, C. A.; Lisensky, G. C. *Inorg. Chem.* **1980**, *19*, 2854.

(14) Workman, M. O.; Dyer, G.; Meek, D. W. *Inorg. Chem.* **1967**, *6*, 1543.

(15) Dyer, G.; Meek, D. W. *Inorg. Chem.* **1967**, *6*, 3983.

(16) Heaney, H.; Millar, I. T. *Org. Synth.* **1973**, *5*, 1120.

Table 1. Experimental Data for the X-ray Crystal Structures of (arom-PSMe)$_2$Ni⁰ (**1**), [(arom-PSMe)$_2$Ni](BF$_4$)$_2$ ([**2**](BF$_4$)$_2$), and (arom-PS)$_2$Ni^{II} (**3**).

complex	1	[2](BF$_4$)$_2$	3
chemical formula	C$_{38}$H$_{34}$P$_2$S$_2$Ni	C$_{38}$H$_{34}$B$_2$F$_8$P$_2$S$_2$Ni	C$_{36}$H$_{28}$P$_2$S$_2$Ni
formula weight (g/mol)	675.4	849.04	645.4
space group	monoclinic	monoclinic	monoclinic
	C2/c	P2$_1$/c	P2$_1$/c
a (Å)	11.467(2)	9.417(4)	9.651(2)
b (Å)	17.613(3)	14.822(9)	12.971(8)
c (Å)	15.733(2)	13.773(2)	12.540(2)
β (deg)	96.450(10)	98.55(3)	110.46(2)
V (Å$^{3)}$)	3157.5(9)	9101(14)	1470.7(11)
Z	4	2	2
ρ(calcd) (g cm^{-3})	1.421	1.483	1.457
temp (K)	193	293	293
radiation		Mo Kα (λ = 0.710 73 Å)	
abs coeff (C m^{-1})	8.70	7.72	9.30
min/max trans coeff	0.9579/0.9857	0.637/0.999	difabs
R (%)^a	6.50	5.18	7.46
wR (%)^a	5.60	12.57	8.96

^{a} Residuals: $R = \sum|F_o - F_c|/\sum F_o$; $wR = \{[\sum w(F_o - F_c)^2]/[\sum w(F_o)^2]\}^{1/2}$.

8H). ^{31}P{^{1}H} NMR (CDCl$_3$): δ 56.1. Anal. Calcd for NiP$_2$S$_2$-C$_{36}$H$_{28}$B$_2$F$_8$ (found): C, 67.0 (66.0); H, 4.34 (4.26).

Bis[*o*-(diphenylphosphino)thioanisole]hydridonickel(II) Tetrafluoroborate ([(H)(arom-PSMe)$_2$Ni](BF$_4$), 4). To a flask containing 0.2 g (0.24 mmol) of [**2**](BF$_4$)$_2$ and a Na/Hg amalgam (15.0 mg of Na in 1 mL of Hg) was added 25 mL of benzene. The solution was vigorously stirred until the nickel complex was reduced, resulting in a color change from yellow to deep red. The red solution was filtered through degassed Celite and placed in an ice bath. A stoichiometric amount of HBF$_4$·Et$_2$O in 10.0 mL of diethyl ether was added to the solution, resulting in a color change from red to clear at the end of addition concomitant with the precipitation of an orange solid. The orange solid was filtered and washed with 20.0 mL of benzene followed by 2 × 15.0 mL of diethyl ether and dried under vacuum to yield 0.10 g (94%) of **4**. ^{1}H NMR (CD$_3$COCD$_3$): δ 8.00−7.45 (m, phenyl, 28 H), 2.15 (s, SCH$_3$, 3 H), −16.19 (t, J_{P-H} = 45.0 Hz, Ni−H, 1 H). ^{31}P{^{1}H} NMR (CD$_3$CN): δ 44.3.

Photolysis of 1. Under an Ar atmosphere, 40.0 mg (0.060 mol) of **1**, obtained from chemical reduction of [**2**](BF$_4$)$_2$, in 25 mL of THF was transferred via cannula to a 100 mL water-jacketed photochemical reaction vessel. Photolysis (15 min with a 450 W mercury vapor lamp) of the solution resulted in a color change from deep red to green, from which 30.0 mg (78%) of (arom-PS)$_2$Ni^{II}, **3**, was recovered. The ^{1}H NMR spectrum of the photolyzed solution of **1** in C$_6$D$_6$ showed the growth of a single resonance of ethane at 0.85 ppm with a decrease of resonance for complex **1**.

Photolysis of 1 with 2,2,6,6-Tetramethyl-1-piperidinyloxy (TEMPO). To a ^{1}H NMR tube was added a solution of 14.0 mg (0.021 mmol) of **1** and 7.0 mg (0.044 mmol) of TEMPO in 1 mL of benzene-d_6. The red solution was photolyzed for 15 min. The resultant yellow-green solution was examined with ^{1}H NMR which showed the formation of 2,2,6,6-tetramethyl-1-piperidinylmethoxide (TEMPO-Me) and (arom-PS)$_2$Ni^{II}, **3**. The solution was filtered through silica gel, dried, and extracted with THF. The organic product was identified by ^{1}H NMR and GC/MS. ^{1}H NMR (C$_6$D$_6$) of TEMPO-Me: δ 3.60 (s, OCH$_3$, 3 H), 1.55−1.25 (m, CH$_2$CH$_2$CH$_2$, 6 H), 1.20 (s, CH$_3$ 12 H). Mass spectrum: m/z (relative intensity) 171 (9) [M]$^+$, 156 (100) [M − CH$_3$]$^+$, 125 (7), 109 (32), 100 (20), 97 (17), 88 (60), 82 (20), 69 (80), 56 (95), 55 (99).

Photolysis of a Mixture of 1 and 1-d_6. To a ^{2}H NMR tube (i.d. = 10 mm) was added a solution of 10.0 mg (14.8 mmol) of **1** and 10.0 mg (14.7 mmol) of **1-d_6** in 3 mL of benzene-d_6. This red solution was irradiated under He atmosphere for 15 min which produced a green solution. The ^{2}H NMR spectrum due to CH$_3$CD$_3$ (s, 0.73 ppm) and CD$_3$CD$_3$ (s, 0.69 ppm) was observed. These gases were flushed by bubbling the reaction solution with He, passed through a glass tube in a dry ice/acetone bath, and finally entrapped in a trap immersed in liquid N$_2$. Immediately, the collected gases were analyzed by a VG Analytical 70S mass spectrometer. The green solution was filtered and dried under vacuum to give 18.0 mg (95%) of a green solid of **3**.

D. X-ray Structure Determination. X-ray quality crystals of **1** were grown by diffusion of methanol into acetonitrile and benzene (method b) or from **1** produced in acetonitrile solution by deprotonation of [(H)(arom-PSMe)$_2$](BF$_4$) with triethylamine. Orange crystals of [**2**](BF$_4$)$_2$ were crystallized from acetone/diethyl ether and green crystals of **3** from CH$_2$Cl$_2$/methanol. Preliminary examination and data collection for **1** and [**2**](BF$_4$)$_2$ were performed on a Siemens R3m/V X-ray diffractometer with an oriented graphite monochromator; for **3** a Rigaku AFC5R X-ray diffractometer with an oriented graphite monochromator was used. Both instruments used Mo Kα radiation (λ = 0.710 73 Å). Diffractometer control software P3VAX 3.42 was supplied by Siemens Analytical Instruments, Inc. All crystallographic calculations were performed with use of the Siemens SHELXTL-PLUS program package. The structures were solved by direct methods and refined using a full-matrix least-squares anisotropic refinement for all non-hydrogen atoms. Carbon-bound hydrogen atoms were placed in idealized positions with isotropic thermal parameters fixed at 0.08 Å. Summaries of the X-ray crystallographic experimental data are given in Table 1.

Results and Discussion

Synthesis and Properties of the Free Ligand and Ni^{II} and Ni⁰ Complexes. The bidentate ligand arom-PSMe was first prepared and used in the synthesis of transition metal complexes by Livingstone and co-workers, and later by others.$^{3a,c−e,5}$ We find that the use of KI instead of CuBr in the synthesis of *o*-halothioanisole in the first step^{16} of the ligand synthesis and the subsequent use of *o*-iodothioanisole for introduction of the PPh$_2$ group leads to products of higher purity and yield, eq 4.
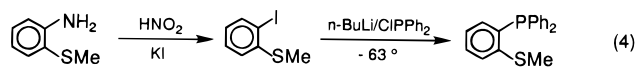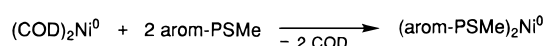

The thioether complex [**2**](BF$_4$)$_2$, prepared according to eq 3,^{6,17} precipitated from a mixture of 2-propanol and THF as a yellow solid. X-ray quality crystals were obtained from acetone/diethyl ether as orange parallelepipeds that are soluble in CH$_3$CN and acetone. The ^{1}H and ^{13}P{^{1}H} NMR and UV/vis spectral data for [**2**](BF$_4$)$_2$ are summarized in Table 2. These spectroscopic parameters are solvent dependent, probably indicative of solvent or counterion interactions at nickel, the most dramatic of which is shown by the ^{31}P{^{1}H} NMR spectra of [**2**](BF$_4$)$_2$. In CD$_2$Cl$_2$ solution the ^{31}P{^{1}H} chemical shift of 51.8 ppm is typical of other four-coordinate Ni^{II} complexes with P,S-donor

(17) Rigo, P.; Bressan, M.; Basato, M. *Inorg. Chem.* **1979**, *18*, 860.
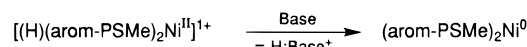
Table 2. ^{31}P and ^{1}H NMR Data (ppm) and UV/Vis Band Positions (nm) for Solutions of arom-PSMe Ligand and Nickel(0) and Nickel(II) derivatives.

complex	^{1}H NMR	^{31}P NMR	UV/Vis[d,e]
arom-PSMe[a]	2.43 (s, 3H), 6.73~6.81 (m, 1H), 6.99~7.13 (m, 1H), 7.22~7.40 (m, 12H)	−14.4	298 (3580)
(arom-PSMe)$_2$Ni^0 (**1**)[b]	2.18 (s, 6H), 6.80~7.80 (m, 20H)	43.8	284 (2320)
			394 (1120, sh)
[(arom-PSMe)$_2$Ni](BF$_4$)$_2$ ([**2**](BF$_4$)$_2$)[c]	2.48(s, 6H), 6.70~8.14 (m, 20H)	−13.0	308 (5090)
			370 (1430, sh)
(arom-PS)$_2$Ni^{II} (**3**)[a]	6.85~7.70 (m, 28H)	56.1	298 (25 560)
			424 (2850)
[(H)(arom-PSMe)$_2$Ni](BF$_4$) (**4**)[c]	−16.20 (t, J_{P-H} = 45 Hz, 1H), 2.17 (s, 6H), 7.45~8.00 (m, 20H)	44.3	284 (1540)
			346 (840, sh)

[a] In CDCl$_3$. [b] In C$_6$D$_6$. [c] In CD$_3$CN. [d] Data taken in corresponding proton solvents., i.e., CHCl$_3$, C$_6$H$_6$, and CH$_3$CN. [e] ϵ is given in parentheses.

Scheme 1

A) Chemical Reduction of Ni^{II} Derivatives

$$[(\text{arom-PSMe})_2\text{Ni}^{II}]^{2+} \xrightarrow{\text{Na / Hg}} (\text{arom-PSMe})_2\text{Ni}^0$$
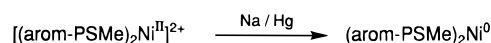
B) Ligand Replacement Reaction of (COD)$_2$Ni^0

$$(\text{COD})_2\text{Ni}^0 + 2\ \text{arom-PSMe} \xrightarrow[-2\ \text{COD}]{} (\text{arom-PSMe})_2\text{Ni}^0$$

C) Deprotonation of Nickel Hydrides

$$[(\text{H})(\text{arom-PSMe})_2\text{Ni}^{II}]^{1+} \xrightarrow[-\text{H:Base}^+]{\text{Base}} (\text{arom-PSMe})_2\text{Ni}^0$$

atom ligands (typically around 50 ppm),[6,17,18] whereas in CD$_3$CN solution, a very broad resonance is barely discernible at −13.0 ppm (indicative of free ligand). Incremental additions of CD$_2$Cl$_2$ to the CD$_3$CN solution of [**2**](BF$_4$)$_2$ resulted in the broadening of the resonance at 52 ppm, with growth of the high-field −13.0 ppm resonance. Broad resonances are expected to arise from complex/ligand exchange; however, the presence of line-broadening hexacoordinate paramagnetic solvates cannot be ruled out. Similar indications of ligand loss or paramagnetic species in CD$_3$CN are indicated by the ^{1}H NMR spectrum of [**2**](BF$_4$)$_2$.

The synthesis of the thiolate complex **3** was best achieved by thermal demethylation of the thioether nickel iodide complex, eq 5. Such nucleophilic demethylation is the reverse of the

$$2\ \text{arom-PSMe} + \text{NiI}_2 \xrightarrow[\Delta\ 2\text{hr}]{\text{EtOH}} (\text{arom-PS})_2\text{Ni}^{II} + 2\ \text{MeI}$$
$$\searrow \qquad\qquad [(\text{arom-PSMe})_2\text{Ni}](\text{I})_2 \qquad\qquad \nearrow \qquad (5)$$
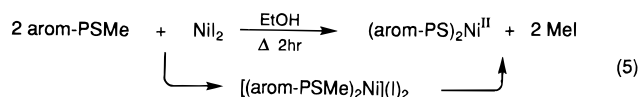
route used to prepare nickel-bound thioethers in N$_2$S$_2$Ni complexes.[19] The green solid obtained from reaction 5 is soluble in CH$_2$Cl$_2$ and CH$_3$Cl, and is surprisingly stable in both acids and bases. Characteristic ^{1}H and ^{13}P{^{1}H} NMR and UV/vis spectral features for **3** are listed in Table 2.

Three synthetic methods (Scheme 1) were used for the preparation of nickel(0) complexes with P,S-donor ligands. Chemical reduction of Ni^{II} by Na/Hg amalgam has been successful for [(PSEt)$_2$Ni](BF$_4$)$_2$ (PSEt = Ph$_2$P(CH$_2$)$_2$SCH$_2$CH$_3$) and [(PSSP)Ni](BF$_4$)$_2$ (PSSP = Ph$_2$P(CH$_2$)$_2$S(CH$_2$)$_3$S(CH$_2$)$_2$-Ph$_2$), producing (PSEt)$_2$Ni^0 and (PSSP)Ni^0, respectively.[6] The Ni(COD)$_2$ has been extensively used for the synthesis of a variety of nickel(0) complexes since the 1,5-cyclooctadiene ligands are easily replaced.[20] Triethylamine (pK_a = 12.0)[21] is

a suitable base for deprotonation of **4**,[22] also leading to **1**. Methods A and B have provided the nickel(0) complex **1** in good yield and high purity, while method C was more successful in the production of X-ray quality crystals.

Complex **1** is somewhat air sensitive as a solid and very air sensitive in solution, decomposing to uncharacterizable products. It dissolves in benzene and toluene to form red solutions, but is insoluble in polar solvents such as methanol and acetonitrile. The ^{1}H NMR and ^{31}P{^{1}H} NMR spectra recorded in CDCl$_3$ show a singlet for the methyl protons at 2.18 ppm and for phosphorus at 43.8 ppm, respectively, Table 2. Protonation of the solution of the nickel(0) complex by HBF$_4$ leads to formation of the hydride complex [(arom-PSMe)$_2$(H)Ni]BF$_4$ (**4**).[23]

Crystal Structures of (arom-PSMe)$_2$Ni^0 (1), [(arom-PSMe)$_2$Ni](BF$_4$)$_2$ ([2](BF$_4$)$_2$), and (arom-PS)$_2$Ni^{II} (3). The molecular structures of **1**, [**2**]$^{2+}$, and **3** are shown in Figures 1−3, respectively, and selected bond distances and angles are compared in Table 3. As in crystal structures of four-coordinate nickel(0) complexes ligated by mixed ligand sets of CO, PR$_3$, and olefins,[25] **1** can best be described in terms of distorted tetrahedral geometry. The S−Ni−P bite angle of **1** is 90.5(1)°, whereas the S−Ni−P(1a) angle between ligands is 118.0(1)°. Likewise the P−Ni−P(1a) angle of 126.9(1)° and S−Ni−S(1a) angle of 115.4(1)° in complex **1** are irregular; however, the angle

(21) Gordon, A. J. *The Chemist's companion*; John Wiley & Sons: New York, 1972; p 60.

(22) (a) Pearson, R. G. *Chem. Rev.* **1985**, *85*, 41. (b) Norton, J. R.; Krisjansdottir, S. S. Acidity of Hydrido Transition Metal Complexes in Solution. In *Transition Metal Hydrides*; Dedieu, A., Ed.; VCH: New York, 1991; p 309.

(23) Upon addition of a stoichiometric amount of HBF$_4$ (diluted in diethyl ether) to a red solution of **1**, prepared from either the chemical reduction of Ni^{2+} derivatives with Na/Hg amalgam or ligand replacement of Ni(COD)$_2$ in benzene solution, an immediate color change occurred from deep red to colorless, precipitating an orange-yellow solid (eq 6).

$$(\text{arom-PSMe})_2\text{Ni}^0 \xrightarrow{\text{HBF}_4} [(\text{H})(\text{arom-PSMe})_2\text{Ni}](\text{BF}_4) \qquad (6)$$
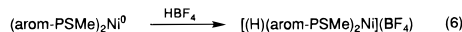
Efforts to grow a single crystal of this hydride complex in solution were fruitless even at low temperature. However, spectroscopic results are almost identical to those structurally characterized [(H)(PSSP)Ni]$^+$ complex.[6,24] The ^{13}P{^{1}H} NMR spectrum recorded in CD$_3$CN exhibits a singlet at 44.3 ppm, while in the ^{1}H NMR spectrum the hydride complex has a triplet at −16.2 ppm (J_{P-H} = 45 Hz) attributable to a metal hydride coupled to two phosphorus atoms and a singlet of methyl protons at 2.17 ppm (Table 2). The ^{1}H NMR spectral resonances of **4** are temperature independent down to −78 °C.

(24) (a) Chojnacki, S. S. Ph.D. Thesis, University of Texas A&M, 1993; p 60. (b) Chojnacki, S. S.; Kim, J. S.; Hsiao, Y. M.; Reibenspies, J. H.; Darensbourg, M. Y. To be submitted to *Inorg. Chem.* for publication.

(25) (a) Sacconi, L.; Ghilardi, C. A.; Mealli, C; Zanobini, F. *Inorg. Chem.* **1975**, *14*, 1380. (b) Sheldrick, W. S. *Acta Crystallogr., Sect. B* **1975**, *31*, 305. (c) Krüger, C.; Tsay, Y. H. *Acta Crystallogr., Sect. B* **1972**, *28*, 1941. (d) Brauer, D. J.; Krüger, C. *J. Organomet. Chem.* **1974**, *77*, 423. (e) Bennett, M. A.; Chiraratvatana, C.; Robertson, G. B.; Tooptakong, U. *Organometallics* **1988**, *7*, 1394. (f) Nickel, T.; Goddard, R.; Krüger, C.; Pörschke, K.-R. *Angew. Chem., Int. Ed. Engl.* **1994**, *33*, 879. (g) Maekawa, M.; Munakata, M.; Kuroda-Sowa, T.; Hachiya, K. *Inorg. Chim. Acta* **1994**, *227*, 137. (h) White, S. G.; Stephan, D. W. *Organometallics* **1988**, *7*, 903.
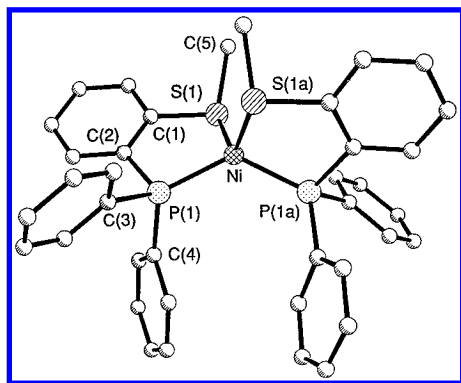
(18) Kyba, E. P.; Davis, R. E.; Fox, M. A.; Clubb, C. N.; Liu, S.-T.; Reitz, G. A.; Scheuler, V. J.; Kashyap, R. P. *Inorg. Chem.* **1987**, *26*, 1647.

(19) (a) Mills, D. K.; Darensbourg, M. Y.; Reibenspies, J. H. *Inorg. Chem.* **1990**, *29*, 4364. (b) Farmer, P. J.; Reibenspies, J. H.; Lindahl, P. A.; Darensbourg, M. Y. *J. Am. Chem. Soc.* **1993**, *115*, 4665.
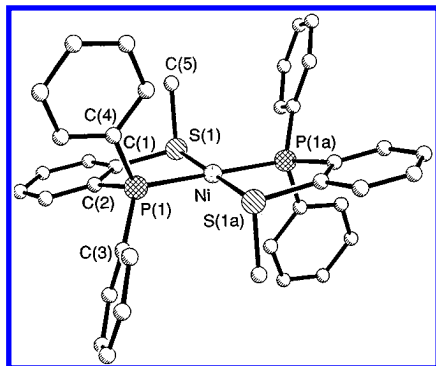
(20) Ittel, S. D. *Inorg. Synth.* **1990**, *28*, 95.

Figure 1. Ball and stick drawing of the molecular structure of (arom-PSMe)$_2$Ni^0 (**1**).

Figure 2. Ball and stick drawing of the molecular structure of [(arom-PSMe)$_2$Ni](BF$_4$)$_2$ ([**2**](BF$_4$)$_2$).
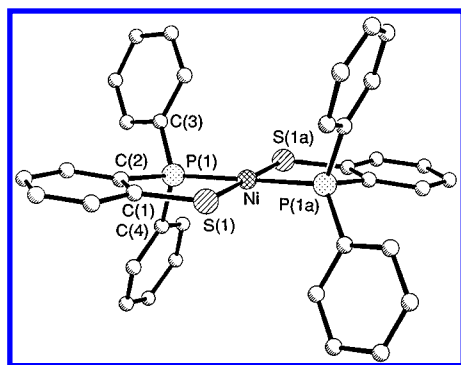

Figure 3. Ball and stick drawing of the molecular structure of (arom-PS)$_2$Ni^{II} (**3**).

between the normals of the planes defined by S$_2$Ni and P$_2$Ni is 92°. The S−arom−P unit is substantially planar; the dihedral angle of S(2)−C(1)−C(2)−P(1) is only 6°. Although other Ni(0) complexes of bidentate and tetradentate phosphino thio-ethers are known and, on the basis of solution spectroscopic data, have been suggested to be of tetrahedral geometry, to our knowledge this is the first crystal structure of such a complex.[6,17,25]

As indicated by the S−Ni−S(1a) and P−Ni−P(1a) angles of 180.0°, both complexes [**2**]$^{2+}$ and **3** are strictly square planar with phosphorus and sulfur atoms *trans* to each other. Comparable thioether and thiolate complexes [(PSEt)$_2$Ni]$^{2+}$ and (PS)$_2$Ni^{II} (PS = Ph$_2$PCH$_2$CH$_2$S$^-$) also have square planar geometries.[6,2e] In both [**2**]$^{2+}$ and **3**, the S−Ni−P angles within the chelate ring are only slightly smaller than the S−Ni−P(1a) angles between ligands, in contrast to pseudotetrahedral **1**. The Ni−S distances diminish in the order **1** > [**2**]$^{2+}$ > **3**. Perhaps surprisingly, the Ni−P distance of complex **1**, 2.143(2) Å, is *shorter* than that of [**2**]$^{2+}$, 2.217(2) Å, or **3**, 2.173(3)Å. The reversal in the order of Ni−L distances (Ni−S > Ni−P in

Table 3. Selected Bond Distances and (Å) and Bond Angles (deg) for (arom-PSMe)$_2$Ni^0 (**1**), [(arom-PSMe)$_2$Ni](BF$_4$)$_2$ ([**2**](BF$_4$)$_2$), and (arom-PS)$_2$Ni^{II} (**3**)

	1	2	3
	Bond Distances		
Ni−S	2.205(2)	2.180(2)	2.166(3)
Ni−P	2.143(2)	2.217(2)	2.173(3)
S(1)−C(1)	1.803(6)	1.778(5)	1.78(1)
S(1)−C(5)	1.814(7)	1.820(5)	
P(1)−C(2)	1.841(6)	1.803(5)	1.809(9)
P(1)−C(3)	1.857(6)	1.813(4)	1.811(9)
P(1)−C(4)	1.827(6)	1.814(4)	1.80(1)
C(1)−C(2)	1.397(8)	1.398(6)	1.36(1)
	Bond Angles		
S(1)−Ni−P(1)	90.5(1)	88.49(5)	88.7(1)
S(1)−Ni−P(1a)	118.0(1)	91.51(5)	91.3(1)
S(1)−Ni−S(1a)	115.4(1)	180.0	180.0(1)
P(1)−Ni−P(1a)	126.9(1)	180.0	180.0(1)
Ni−S(1)−C(1)	104.7(2)	106.6(2)	107.2(3)
Ni−S(1)−C(5)	119.6(3)	105.5(2)	
Ni−P(1)−C(2)	104.7(2)	106.5(2)	107.5(3)
Ni−P(1)−C(3)	125.2(2)	118.5(2)	113.6(3)
Ni−P(1)−C(4)	120.3(2)	112.9(2)	119.5(3)
S(1)−C(1)−C(2)	116.6(4)	119.8(3)	119.5(8)
P(1)−C(2)−C(1)	118.5(4)	115.8(3)	116.0(8)

complex **1**; Ni−S < Ni−P in complexes [**2**]$^{2+}$ and **3**) possibly reflects the better match of the soft/soft interaction of Ni(0) and P in **1** vs the borderline hard/borderline soft interactions of Ni(II) and S in complexes [**2**]$^{2+}$ and **3**. In complex [**2**]$^{2+}$ the Ni−S distance of 2.180(2) Å is slightly shorter than those of the four-coordinate Ni(II) complexes with phosphino thioether sites bridged by CH$_2$CH$_2$: 2.208 Å for [(PSEt)$_2$Ni](BF$_4$)$_2$ and 2.213 Å for [(PSSP)Ni](ClO$_4$)$_2$.[6,26] This is consistent with a strengthening of the Ni−S$_{arom}$ bond as compared to the Ni−S$_{alkyl}$ bond.

It should be noted that complex **3** has been synthesized by other groups as well as ourselves, and isolated as green crystals.[2a,b] In fact, an earlier crystal structure of complex **3** was reported by Zubieta and co-workers in a series of structures of square planar nickel complexes.[27] That structure was, however, taken on a brown crystal and displayed crystal data different from those of other members of the series as well as our own complex **3** and known group VIII metal dithiolate complexes, i.e., (arom-PS)$_2$Pd^{II} and (PS)$_2$Ni^{II}.[2e,6] The source of this discrepancy is not clear.

Electrochemistry. The cyclic voltammogram of [**2**](BF$_4$)$_2$ shows two redox couples, Figure 4. On the basis of EPR results, *vide infra*, the first redox couple is assigned to Ni$^{II/I}$ and the second event to Ni$^{I/0}$. As the sweep rate increases from 100 to 500 mV/s, the peak separation of the Ni$^{II/I}$ couple increases from 129 to 239 mV, indicative of a quasi-reversible electrochemical process, discussed further below. In contrast, the Ni$^{I/0}$ couple is fully reversible.[28] Table 4 compares the electrochemical data for [**2**](BF$_4$)$_2$ to results of bidentate [(PSEt)$_2$Ni](BF$_4$)$_2$ and tetradentate [(PSSP)Ni](BF$_4$)$_2$ derivatives, which show the same CV features.[28]

Scheme 2 delineates the differences in the stabilization of reduced nickel as dependent on the P−S linking group; $E_{1/2}$ values are referenced to NHE. The poorer electron donating ability of arom-PSMe ligand provides easier access to Ni^I and

(26) Aurivillius, K.; Bertinsson, G. -I. *Acta Crystallogr.* **1981**, *B37*, 72.

(27) Block, E.; Ofori-Okai, G.; Kang, H.; Zubieta, J. *Inorg. Chim. Acta* **1991**, *188*, 7.

(28) The redox potentials for Ni^{II} complexes which were reported in ref 6 have been calibrated to ferrocenium (Cp$_2$FePF$_6$, $E_{1/2}$ = 400 mV) in order to compare with the potentials reported here: +400 mV for (PS)$_2$Ni^{II}; −280 mV (ΔE = 117 mV) and −901 mV (ΔE = 101 mV) for Ni$^{II/I}$ and Ni$^{I/0}$, respectively, of [(PSEt)$_2$Ni](BF$_4$)$_2$; −347 mV (ΔE = 125 mV) and −894 mV (ΔE = 63 mV) for Ni$^{II/I}$ and Ni$^{I/0}$, respectively, of [(PSSP)Ni](BF$_4$)$_2$.
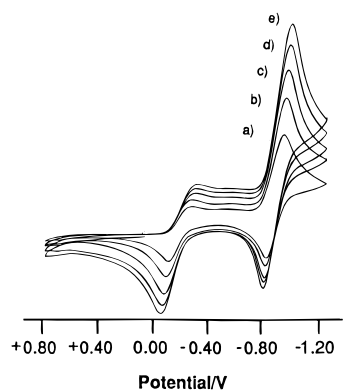
Figure 4. Cyclic voltammograms of a 1.5 mM solution of [(arom-PSMe)$_2$Ni](BF$_4$)$_2$ ([**2**](BF$_4$)$_2$). Scans toward negative potential using a glassy carbon working electrode at (a) 100, (b) 200, (c) 300, (d) 400, and (e) 500 mV/s (scale referenced to Ag/AgNO$_3$ and calibrated for ferrocene).

Table 4. Electrochemical Data[a]

complex		E_{pc} (mV)	E_{pa} (mV)	$E_{1/2}$ (mV) (ΔE_p (mV))
1[b]	Ni$^{II/I}$		78	
	Ni$^{I/0}$	−859	−770	−815 (89)
[**2**](BF$_4$)$_2$[b]	Ni$^{II/I}$	−138	−49	−93 (89)
	Ni$^{I/0}$	−831	−738	−784 (93)
3[c]	Ni$^{II/III}$	702	638	670 (64)
[(PSEt)$_2$Ni](BF$_4$)$_2$[d]	Ni$^{II/I}$	−221	−339	−280 (118)
	Ni$^{I/0}$	−850	−952	−901 (102)
[(PSSP)Ni](BF$_4$)$_2$[d]	Ni$^{II/I}$	−284	−410	−347 (126)
	Ni$^{I/0}$	−862	−926	−894 (63)

[a] All potentials calibrated for ferrocene are recorded with a vitreous carbon disk working electrode and 0.1 M [n-Bu$_4$N][PF$_6$] as a supporting electrolyte vs the Ag/0.01 M AgNO$_3$ reference electrode. The potential scan rate is 200 mV/s. [b] CH$_3$CN. [c] CH$_2$Cl$_2$. [d] Reference 24.

Scheme 2

Figure 5. Cyclic voltammograms of (a) a 1.0 mM solution of (arom-PSMe)$_2$Ni^0 (**1**) in 0.1 M [(n-Bu)$_4$N][PF$_6$]/CH$_3$CN and (b) a 1.0 mM solution of (arom-PS)$_2$Ni^{II} (**3**) in 0.1 M [(n-Bu)$_4$N][PF$_6$]/CH$_2$Cl$_2$. Scans toward negative potential using a glassy carbon working electrode at 200 mV/s (scale referenced to Ag/AgNO$_3$ and calibrated for ferrocene).

Ni$^{I/0}$ couple is greater by a factor of 2 for the P to S aromatic linkage relative to CH$_2$CH$_2$. A further destabilization is realized on linking the thioether donors; this is attributed to steric restriction or impedance to the rearrangement needed as the geometrical preference of reduced nickel changes from square planar to tetrahedral.

The electrochemical data found in Table 4 show some irreversibility of the Ni$^{II/I}$ couple as compared to the typically reversible Ni$^{I/0}$ couple in the nickel(II) complexes [**2**](BF$_4$)$_2$, [(PSEt)$_2$Ni](BF$_4$)$_2$, and [(PSSP)Ni](BF$_4$)$_2$. The current ratio of the Ni$^{II/I}$ couple ($i_{pa}/i_{pc} \approx 1.4$) of [**2**](BF$_4$)$_2$ is assumed to reflect the fact that electron transfer is coupled to a structural change of the Ni^I species. Such structural changes of complexes that accompany electron transfer have been reviewed by Geiger,[30] and general results are consistent with those seen here. That is, consumption of one electron by the nickel(II) complex [**2**](BF$_4$)$_2$ produces a nickel(I) species of structure close to that of the original square planar nickel(II) complex, and subsequently, a tetrahedral twist of this intermediate yields a nickel(I) species close in structure to the tetrahedral nickel(0) complex **1**. The distorted tetrahedral structure of the Ni^I complex has been previously suggested for bidentate phosphine and macrocyclic tetradentate P,S donor ligands from similar electrochemical data.[31,32] Interestingly, the second reduction, the Ni$^{I/0}$ couple of [**2**](BF$_4$)$_2$, is scan rate independent and fully reversible ($i_{pa}/i_{pc} \approx 1.0$), indicating that the major structural change has occurred following addition of the first electron.

Shown in Figure 5a is the cyclic voltammogram of complex **1** recorded in CH$_3$CN. Electrochemically, the cyclic voltammogram features of the nickel(0) complex should be the same as those of the nickel(II) complex, [**2**](BF$_4$)$_2$. However, the low

Ni^0 species relative to the PSEt and PSSP ligands. (This generalization is also demonstrated in the electrochemistry of free phosphines. The $E_{1/2}$ for the oxidation of the free phosphine ligand increases with increasing phenyl substitution.)[29] Scheme 2 also shows that stabilization of the Ni$^{II/I}$ as compared to the
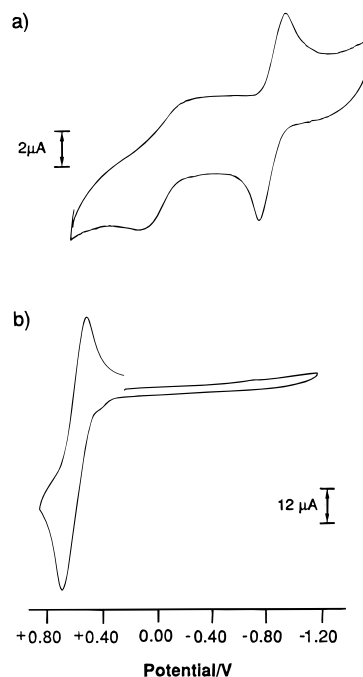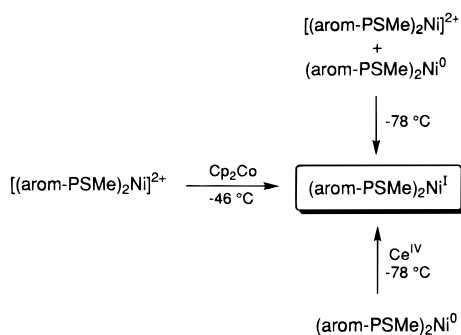
(29) Matschmer, V. H.; Krause, L.; Krech, F. *Z. Allg. Chem.* **1970**, *373*, 1.

(30) Geiger, W. E. *Prog. Inorg. Chem.* **1985**, *33*, 275.

(31) Martelli, M.; Pilloni, G.; Zotti, G.; Daolio, S. *Inorg. Chim. Acta* **1974**, *11*, 155.

(32) Kyba, E. P.; Davis, R. E.; Fox, M. A.; Clubb, C. N.; Liu, S.-T.; Reitz, G. A.; Scheuler, V. J.; Kashyap, R. P. *Inorg. Chem.* **1987**, *26*, 1647.

Scheme 3

Figure 6. EPR spectrum (—) measured at 100 K for the frozen CH$_3$CN solution of (arom-PSMe)$_2$Ni^I prepared by Cp$_2$Co reduction of [**2**](BF$_4$)$_2$ at −46 °C. Overlaid is the EPR spectrum (- - -) measured at 10 K for the solution containing (arom-PSMe)(arom-PS)Ni^I resulting from *S*-dealkylation of complex **1**.

Scheme 4

solubility of **1** in CH$_3$CN leads to more irreversible behavior as well as small current readings. In CH$_2$Cl$_2$, complex **1** is more soluble; however, solution degradation is rapid under electrolytic conditions.

The cyclic voltammogram of **3** is presented in Figure 5b, and displays a reversible one-electron oxidation at 670 mV. Because of its good reversibility, the assignment to Ni$^{II/III}$ (rather than the usual oxidation of thiolate S to the thiyl radical)[6] is tentatively made. No reduction is seen within this solvent window. A similar thiolate nickel complex, (PS)$_2$Ni^{II}, shows an irreversible peak at 400 mV which is presumed to be due to the oxidation of thiolate S to the thiyl radical.[6]

Electron Spin Resonance Studies. Corroboration of the assignment of the single-electron-reduced **2^r**, intermediate from Ni^{II} to Ni^0, to a Ni^I species was provided by EPR spectroscopy. Three bulk chemical synthetic approaches to the nickel(I) complex were used: (a) the reduction of [**2**](BF$_4$)$_2$ with Cp$_2$Co, (b) the oxidation of **1** with Ce^{IV} and, (c) the comproportionation of [**2**](BF$_4$)$_2$ and **1** at low temperature (Scheme 3). All three methods yielded a yellow paramagnetic solution which showed the same EPR spectral characteristics. Shown in Figure 6, for example, is the EPR spectrum obtained upon adding 1.1 equiv of Cp$_2$Co to a red solution of [**2**](BF$_4$)$_2$ in CH$_3$CN at −46 °C and further cooling to 100 K for the analysis.

The spectrum exhibits an axial signal, from which g values $g_x = g_y = 2.10$ and $g_z = 1.96$ are calculated. Each peak is split into three lines of intensity ratio 1:2:1, indicating coupling of the unpaired electron with two equivalent ^{31}P nuclei. The peak to peak widths of the ^{31}P hyperfine coupling on the $g_x = g_y$ and g_z lines are 42 and 45 G, respectively. The concentration of this nickel(I) complex was calculated and compared to the double integral of the EPR spectrum of 1.0 mM Cu^{II} in 10 mM EDTA and shows 61% conversion of [**2**](BF$_4$)$_2$ to (arom-PSMe)$_2$Ni^I. The (arom-PSMe)$_2$Ni^I complex is stable at low temperatures (−46 °C or lower) but decomposes on warming to 22 °C.

A similar EPR spectrum of a nickel(I) complex produced by Cp$_2$Co reduction of [Ni(pspyr)$_2$]$^+$ (where pspyr = 4-(diphenylphosphino)-1-(2-pyridyl)-2-thiabutane) at −55 °C was reported by Holm *et al.*[7] This ligand achieves four-coordinate nickel(I) diphosphino dithioether from six-coordinate nickel(II) on reduction and deligation of the axial nitrogens. The ^{31}P hyperfine coupling is on the order of 40−60 G. In contrast, the EPR spectrum of a Ni^I(PMe$_3$)$_4$$^+$ complex, known from X-ray crystal structure analysis to have a tetrahedral geometry with average P−Ni−P angles of 109°,[33] shows an isotropic, broad resonance with $g = 2.12$ G, and no ^{31}P hyperfine coupling. This suggests that ^{31}P hyperfine coupling with an unpaired electron of Ni^I is highly geometry dependent, a conclusion to be further explored below. Since the cyclic voltammetry studies, *vide infra*,

indicated some structural distortions from the square planar [(arom-PSMe)$_2$Ni]$^{2+}$ as it underwent one-electron reduction, we conclude that the observed ^{31}P coupling is indicative of a geometry intermediate between square planar and tetrahedral for the Ni^I analogue. We do not know the acuteness of the dependence of tetrahedral twist, P$_{d\pi}$−Ni$_{d\pi}$ overlap, and ^{31}P coupling.

***S*-Dealkylation of (Ph$_2$P(o-C$_6$H$_4$)SCH$_3$)$_2$Ni^0.** The nickel(II) complex [**2**](BF$_4$)$_2$ in CH$_3$CN solution was stable to photolysis.[34] However, red solutions of complex **1**, prepared by either chemical reduction of [**2**](BF$_4$)$_2$ in benzene (method A) or deprotonation of hydride complex **4** with Et$_3$N in CH$_3$CN (method C), are light sensitive. Under ambient lighting, the red solution turns green within a day, producing dithiolate complex **3**; under photolytic conditions, 15 min is sufficient. The ^{1}H NMR spectrum of a sample of complex **1**, irradiated for 15 min in C$_6$D$_6$, exhibited resonances for (arom-PS)$_2$Ni^{II}, **3**, as well as a singlet at 0.85 ppm, consistent with the presence of ethane and insinuating the generation of methyl radicals during the decomposition as shown in Scheme 4. No methane was observed either in the NMR spectrum or by gas chromatography on the head gas.

Further evidence of C−S bond cleavage and the production of methyl radicals was provided by photolysis of complex **1** in the presence of the alkyl radical trapping agent TEMPO.[35] As indicated in Scheme 4, complex **3** and 2,2,6,6-tetramethyl-1-

(33) Gleizes, A.; Dartiguenave, M.; Dartiguenave, Y.; Galy, J.; Klein, H. F.; *J. Am. Chem. Soc.* **1977**, *99*, 5187.
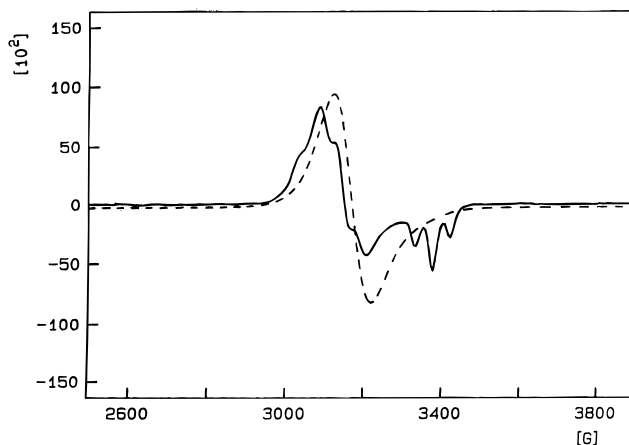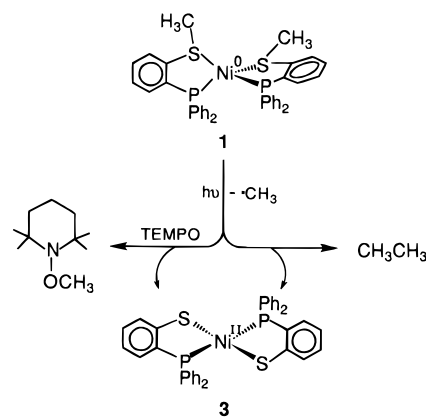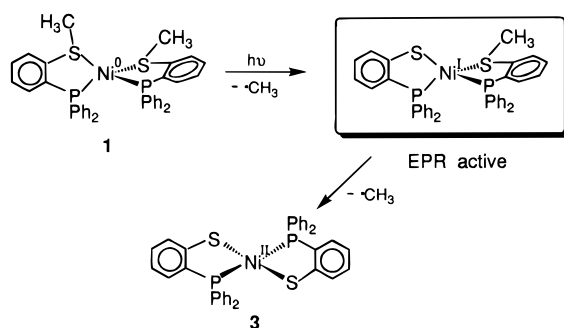
(34) No distinctive chemical change was observed during the photolysis of [**2**](BF$_4$)$_2$ in CH$_3$CN for 1.5 h.
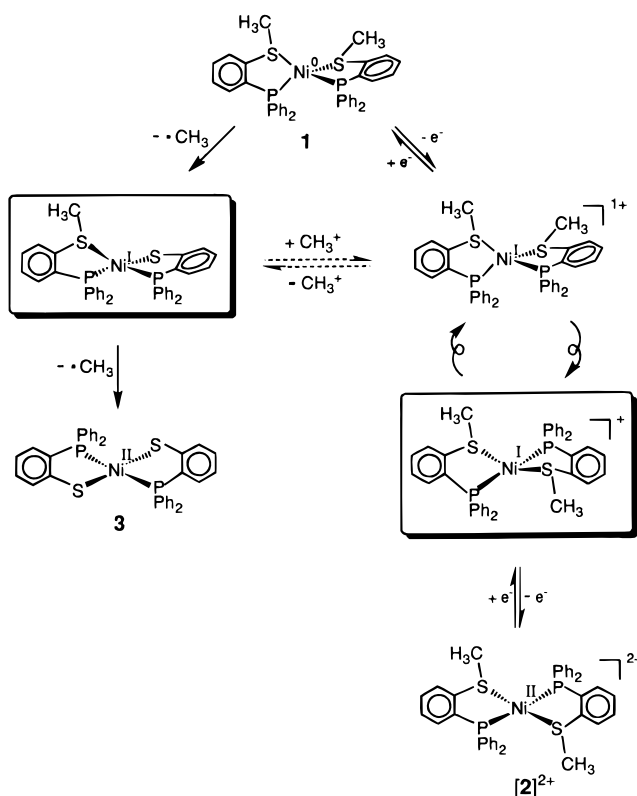
Scheme 5

Scheme 6

piperidinylmethoxide (TEMPO-Me) were produced.[36,37] The control experiment, i.e., a solution of complex **1** (1.0×10^{-2} M) and TEMPO (2.1×10^{-2} M) in the dark, showed no reaction under ambient conditions. In the course of the photochemical reaction of complex **1** with TEMPO, dimerization of methyl radicals or abstraction of hydrogen by the methyl radical has not been observed, which is consistent with relatively large rate constants for nitroxyl radical couplings with primary carbon radicals ($k_{20} = 1.2 \times 10^9$ M^{-1} s^{-1}).[35a,38]

As depicted in Scheme 5, successive homolytic cleavage of the $H_3C-S_{thioether}$ bonds suggests the possibility of an intermediate thioether/thiolate nickel(I) species. EPR spectroscopy was employed as a probe according to the following procedure: A sample of the red solution of **1**, produced by the deprotonation of complex **4** with Et$_3$N in CH$_3$CN, was exposed to laboratory lighting for 30 min, and then cooled to 100 K, and further to 10 K. The EPR spectrum was invariant with temperature, and the same feature was observed repeatedly on additional samples of light-degraded complex **1**. That spectrum, shown in Figure 6, is isotropic with $g = 2.08$, in contrast with that of the anisotropic [(arom-PSMe)$_2$Ni^I]$^+$, which is given for comparison. Also dissimilar to [(arom-PSMe)$_2$Ni^I]$^+$, no ^{31}P hyperfine coupling was detected for (presumably) [(arom-PSMe)(arom-PS)Ni^I]. The structural implications consistent with these EPR data are as follows: The neutral thioether/thiolate Ni^I species has a ground state geometry closer to tetrahedral, affording weaker interactions between the two phosphorus atoms and the unpaired electron on nickel; the cationic dithioether Ni^I species has a ground state geometry sufficiently square planar-like to account for the hyperfine ^{31}P-unpaired electron interaction.
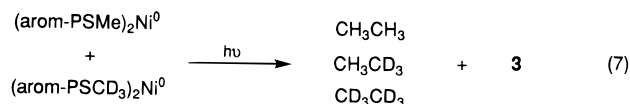
The light-sensitive feature of C–S bonds of thioether ligands upon coordination to nickel(II) has been previously noted by Schrauzer and co-workers.[39] Photolysis of S,S'-diaralkyl nickel(II) derivatives yields neutral thiolate nickel(II) complexes and organic products derived from carbon radicals. The formation of nickel metal-based paramagnetic species in this reaction was subsequently confirmed by EPR studies.[40]

Organic Products Resulting from Photolytic S-Dealkylation. The observation of ethane during the photolysis of **1** prompts the question of C–C bond formation via an inter- or intramolecular mechanism. To this end, the arom-PSMe ligand was substituted with CD$_3$ and a deuterated nickel(0) derivative, (arom-PSCD$_3$)$_2$Ni^0 (**1-d_6**), was prepared. Formation of CD$_3$CD$_3$ in the course of irradiation of **1-d_6** in benzene provides an assignment of the chemical shift at 0.69 ppm to CD$_3$CD$_3$ in the ^{2}H NMR spectrum. A 1:1 mixture of **1** and **1-d_6** was photolyzed in benzene-d_6 or benzene, and the products were analyzed by ^{1}H and ^{2}H NMR and mass spectroscopy. Together the ^{1}H and

^{2}H NMR spectra show the production of three ethane isotopomers, CD$_3$CD$_3$, CH$_3$CD$_3$, and CH$_3$CH$_3$, eq 7. The ^{2}H NMR


$$(7)$$

spectrum found ethane-d_6 and ethane-d_3 in a 1:2 ratio; while the ^{1}H NMR spectrum showed ethane and ethane-d_3. The three different ethanes from the mixture were further confirmed by the mass spectrum of the head gas. The results are consistent with an intermolecular combination of methyl radicals.

Concluding Comments

Sulfur dealkylation in reduced nickel and iron complexes of polydentate thioethers has been previously observed by Kovacs et al. and Sellman et al.;[11,12] thus, the photosensitivity of reduced

(36) 2,2,6,6-Tetramethyl-1-piperidinylmethoxide (TEMPO-Me) was analyzed by NMR and GC/MS as described in the Experimental Section. Coinjection of TEMPO and *tert*-butylperoxide into the hot injection port (250 °C) of the GC/mass spectrometer provides authentic TEMPO-Me for comparison.[37]

$$(8)$$
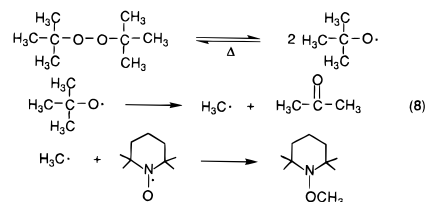
(37) Choo, K. Y.; Benson, S. W. *Int. J. Chem. Kinet.* **1981**, *13*, 833.
(38) Kochi, J. K. In *Free Radical*; Kochi, J. K., Eds.; John Wiley & Sons: New York, 1973; p 680.
(39) (a) Schrauzer, G. N.; Rabinowitz, H. N. *J. Am. Chem. Soc.* **1968**, *90*, 4297. (b) Zhang, C.; Reddy, H. K.; Schlemper, E. O.; Schrauzer, G. N. *Inorg. Chem.* **1990**, *29*, 4100.
(40) Ohtani, M.; Ohkoshi, S.-I.; Kajitani, M.; Akiyama, T.; Sugimori, A.; Yamauchi, S.; Ohba, Y.; Iwaizumi, M. *Inorg. Chem.* **1992**, *31*, 3873.

(35) (a) Newcomb, M. *Tetrahedron* **1993**, *49*, 1151. (b) Sheats, J. R.; McConell, H. M. *J. Am. Chem. Soc.* **1977**, *99*, 7091.

nickel toward S−C bond cleavage exhibited by complex **1** is not without precedent. An interesting feature of this P_2S_2 system however lies in the possibility of interpreting the EPR spectrum of the intermediate Ni^I species in terms of geometry. Clearly d^{10} Ni^0 complexes are expected to be tetrahedral regardless of the donor ligand; d^8 Ni^{II} complexes in P_2S_2 donor environments are square planar, for S = a thiolate or thioether donor. Thus, the geometrical preference of d^9 Ni^I is not clear and, we concur with the statement of Holm et al., "the structural systematics of Ni^I are not extensively developed".[7] The contribution in this regard from our P_2S_2Ni studies is summarized in Scheme 6. The EPR evidence suggests that loss of a single Me• and creation of a neutral, d^9 Ni^I in diphosphino thioether thiolate ligation substantially retains the tetrahedral geometry of the parent Ni^0 complex **1**. In contrast the cationic Ni^I in diphosphino dithioether coordination, although distorted, is sufficiently square planar for an anisotropic EPR spectrum and ^{31}P hyperfine interactions. We can only conclude that delocalization of the odd electron is favored for the dithioether ligand environment in the cationic species and dictates a distorted square planar geometry, whereas electron/thiolate ligand repulsion governs the geometrical preference of the thioether/thiolate ligands, encouraging tetrahedral character. Since the $Ni^I(PMe_3)_4^+$ species is also tetrahedral,[33] the balance of factors is indeed precarious.

Supporting Information Available: Figures showing alternate views and packing diagram of complexes **1**, **2**(BF$_4$)$_2$, and **3** and tables summarizing crystallographic data and refinement, atomic coordination, bond lengths, bond angles, anisotropic displacement parameters, and H atom coordinates (27 pages). This material is contained in many libraries on microfiche, immediately follows this article in microfilm version of the journal, can be ordered from the ACS, and can be downloaded from the Internet; see any current masthead page for ordering information and Internet access instructions.

JA953686H